Stability Analysis of Ships Undergoing Strong Roll Amplifications in Head Seas

Marcelo A. S. Neves, masn@peno.coppe.ufrj.br
Claudio A. Rodríguez, claudiorc@peno.coppe.ufrj.br
(LabOceano, COPPE, Universidade Federal do Rio de Janeiro, Brazil)

ABSTRACT

A new mathematical model with nonlinearities defined up to the third order in terms of the heave, roll and pitch couplings is introduced, in order to simulate strong roll parametric amplifications in head seas. The influence of hull stern shape is discussed. A theoretical analysis discloses some essential dynamical characteristics associated with the proposed coupled third order mathematical model. The influence of nonlinear terms on the dynamics of roll parametric resonance appears to be relevant for low metacentric conditions and extreme waves in the head seas condition.

1. INTRODUCTION

Occurrences of head seas parametric resonance with different ship types have been reported by, among others, France *et al.* (2003), Luth and Dallinga (1999), Palmquist and Nygren (2004). In the case of fishing vessels, head-sea parametric rolling has been discussed in Neves *et al.* (2002). Two small vessels were tested at different speeds, various wave amplitudes, and two metacentric height conditions for each hull. The two vessels have very similar characteristics but their sterns are different. The present study focuses on analyzing, both analytically and numerically, the situations in which parametric resonance was developed during the experiments. During the experiments some conditions showed intense amplification, especially those corresponding to the transom stern hull, in particular when tested in high waves and low metacentric height.

Uncoupled Mathieu and Mathieu-Duffing equations and its variants are mathematical models often used for parametric resonance investigations. It is not uncommon for these models to overpredict the resonant rolling motions observed in experiments, see for instance Umeda *et al* (2003). In fact, the transom stern hull tested by Neves *et al.* (2002) is a good example in which parametric excitation assessed considering terms up to the second order, i.e., using the classical Mathieu type modelling, tends to give excessive excitation.

In order to overcome these deficiencies, a new third order mathematical model which comprehensively couples the heave, roll and pitch motions has been developed, Neves and Rodríguez (2004). Nonlinearities are taken into account in the restoring actions as well as in the roll damping moment. This enhanced model has been implemented numerically and results were compared with experiments showing that it matches better with the experiments than the second order model, even in situations in which strong roll amplifications were reported, Neves and Rodríguez (2004).

In the present paper, the influence of the restoring coefficients (expressed in terms of hull form characteristics, motions and wave

profile) and the corresponding parametric excitation on both ship responses are discussed. The connections between hull forms and roll parametric amplification, which had been discussed previously on the basis of experimental results by Neves *et al.* (2002), are here confirmed and qualified by the analytical results derived from an elaborate coupled non-linear mathematical model.

2. EXPERIMENTAL APPROACH

2.1 Main Characteristics of the Tested Hulls

The main characteristics and the lines plans of the vessels used in the present research are shown in Table 1 and Figure 1, respectively. It may be observed that the two hulls have very similar dimensions and hull characteristics, but different stern arrangements: the hull on the left corresponds to a typical transom stern hull, here denominated TS; and the one on the right is a conventional round stern vessel, which will be called RS.

Table 1. Principal particulars of ships

Denomination	TS	RS
Length overall (m)	25.91	24.36
Length between perpendiculars (m)	22.09	21.44
Beam (m)	6.86	6.71
Depth (m)	3.35	3.35
Draught (m)	2.48	2.49
Displacement (tons)	170.30	162.60
Waterplane area (m^2)	121.00	102.50
Pitch radius of gyration (m)	5.35	5.52

As mentioned above, these vessels have been tested experimentally under parametric rolling in longitudinal regular head-sea waves at the first region of resonance, defined as the condition corresponding to the encounter frequency coinciding with twice the roll natural frequency. Detailed descriptions of all tested conditions can be found in Neves *et al.* (2002).

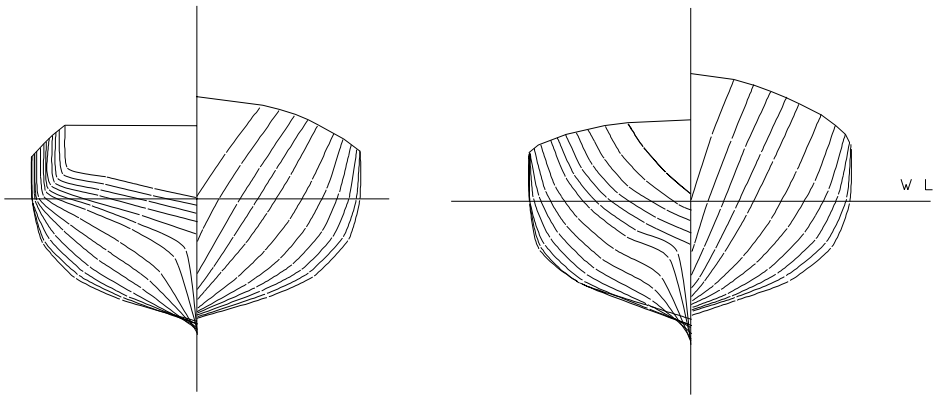

Figure 1 Body plan of tested vessels (TS and RS).

2.2 Analysis of Experimental Results

A summary of the experimental results for the ship RS is presented in Figure 2, in which the steady amplitude of parametric roll is plotted against Froude number, for the two tested metacentric heights. An important feature observed is the decreasing of parametric roll amplitude (when the same wave amplitude is considered) as speed increases, in both *GM* conditions.

In the case of ship TS, analogous plots to those presented above for the ship RS are used – see Fig. 3. It is observed that the variation of roll amplitude with speed is quite different: for the lower *GM* and small Froude numbers there is a tendency for roll angles to vary in a similar way as discussed previously to the RS hull. Yet, for higher speeds, the tendency is reversed, and very large roll angles are obtained (up to 38° for *Fn*=0.30); for the higher *GM* case the same tendency observed in the RS

hull is verified in the whole speed range. Furthermore, in this latter case, it may be noticed that for *Fn* > 0.15 practically no amplification was observed.

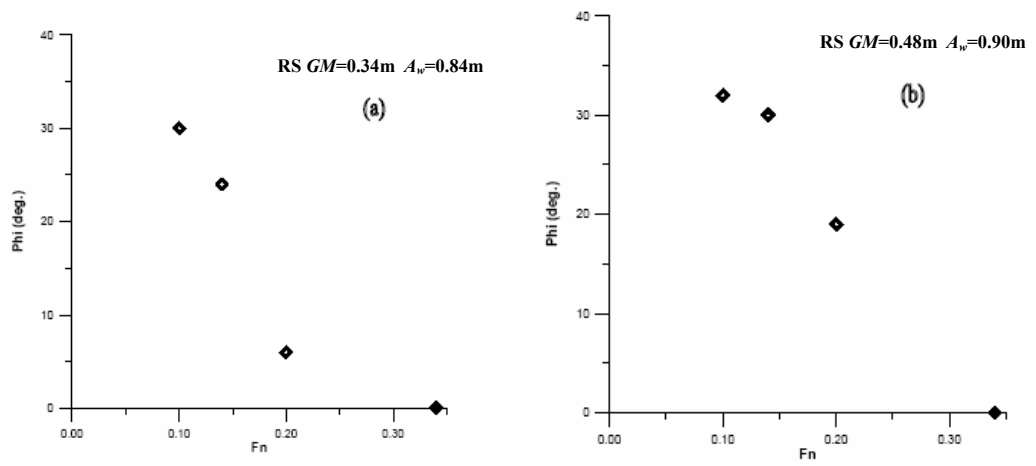

Figure 2 Variation of parametric roll amplitude with Froude number for RS hull: (a) *GM*=0.34m, A_w=0.84 m; (b) *GM*=0.48 m, A_w=0.90 m.

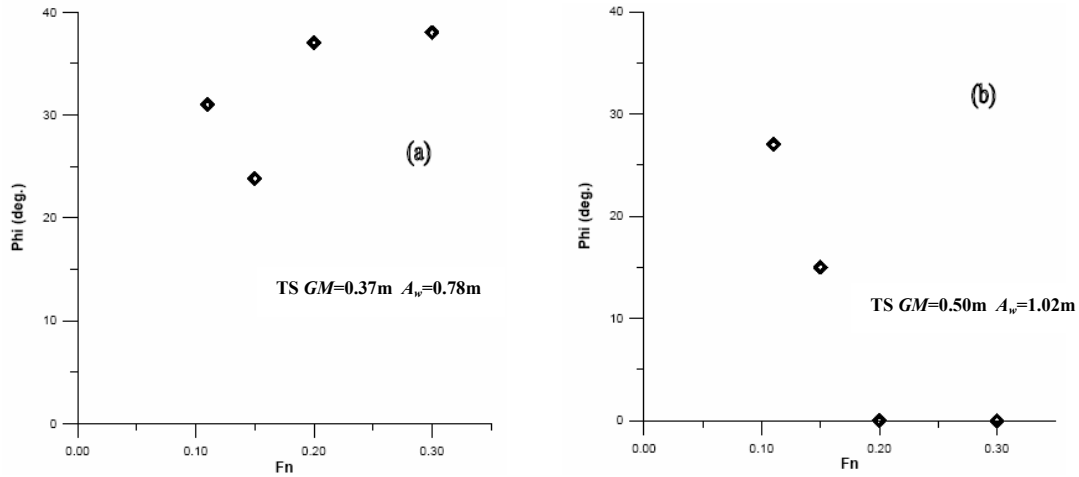

Figure 3 Variation of parametric roll amplitude with Froude number for TS hull: (a) *GM*=0.37m, A_w=0.78 m; (b) *GM*=0.50 m, A_w=1.02 m.

In summary, for the TS hull, low *GM* (*GM*=0.37m) produces intense parametric resonances at all speeds at wave amplitudes of the order of A_w=0.78 m. The other hull, even at a slightly lower metacentric height, *GM*=0.34 m, and larger wave amplitude, A_w=0.90 m, tends to respond less and less for higher speeds. The same TS hull for a high *GM* condition (*GM*=0.50 m) does not amplify parametric excitation at high speeds, indicating that a transom stern shape, together with a low *GM*, has a relevant effect on the tendency for parametric amplification.

3. THEORETICAL APPROACH

3.1 Mathematical Model

As anticipated, the mathematical model used in the present paper couples the equations of motion in heave, roll and pitch, and contemplates nonlinearities up to third order in

the restoring actions and the roll damping moment:

$$(m+Z_{\ddot z})\ddot z+Z_{\dot z}\dot z+Z_{\ddot\theta}\ddot\theta+Z_{\dot\theta}\dot\theta+Z_z z+Z_\theta\theta+\frac{1}{2}Z_{zz}z^2+\frac{1}{2}Z_{\phi\phi}\phi^2+\frac{1}{2}Z_{\theta\theta}\theta^2+Z_{z\theta}z\theta$$
$$+\frac{1}{6}Z_{zzz}z^3+\frac{1}{2}Z_{zz\theta}z^2\theta+\frac{1}{2}Z_{\phi\phi z}\phi^2 z+\frac{1}{2}Z_{\phi\phi\theta}\phi^2\theta+\frac{1}{2}Z_{\theta\theta z}\theta^2 z+\frac{1}{6}Z_{\theta\theta\theta}\theta^3+Z_{\zeta z}(t)z$$
$$+Z_{\zeta 0}(t)\theta+Z_{\zeta\zeta z}(t)z+Z_{\zeta z z}(t)z^2+Z_{\zeta\zeta 0}(t)\theta+Z_{\zeta z\theta}(t)z\theta+Z_{\phi\phi\zeta}(t)\phi^2+Z_{\theta\theta\zeta}\theta^2=Z_w(t)$$

$$(J_{xx}+K_{\ddot\phi})\ddot\phi+K_{\dot\phi}\dot\phi+K_{\dot\phi|\dot\phi|}\dot\phi|\dot\phi|+K_\phi\phi+K_{z\phi}z\phi+K_{\phi\theta}\phi\theta+\frac{1}{2}K_{zz\phi}z^2\phi+\frac{1}{6}K_{\phi\phi\phi}\phi^3$$
$$+\frac{1}{2}K_{\theta\theta\phi}\theta^2\phi+K_{z\phi\theta}z\phi\theta+K_{\zeta\phi}(t)\phi+K_{\zeta\zeta\phi}(t)\phi+K_{\zeta z\phi}(t)z\phi+K_{\zeta\phi\theta}(t)\phi\theta=K_w(t)$$

$$(J_{yy}+M_{\ddot\theta})\ddot\theta+M_{\dot\theta}\dot\theta+M_{\ddot z}\ddot z+M_{\dot z}\dot z+M_z z+M_\theta\theta+\frac{1}{2}M_{zz}z^2+\frac{1}{2}M_{\phi\phi}\phi^2+\frac{1}{2}M_{\theta\theta}\theta^2$$
$$+M_{z\theta}z\theta+\frac{1}{6}M_{zzz}z^3+\frac{1}{2}M_{zz\theta}z^2\theta+\frac{1}{2}M_{\phi\phi z}\phi^2 z+\frac{1}{2}M_{\phi\phi\theta}\phi^2\theta+\frac{1}{2}M_{\theta\theta z}\theta^2 z+\frac{1}{6}M_{\theta\theta\theta}\theta^3$$
$$+M_{\zeta z}(t)z+M_{\zeta 0}(t)\theta+M_{\zeta\zeta z}(t)z+M_{\zeta z z}(t)z^2+M_{\zeta\zeta 0}(t)\theta+M_{\zeta z\theta}(t)z\theta+M_{\phi\phi\zeta}(t)\phi^2$$
$$+M_{\theta\theta\zeta}\theta^2=M_w(t)$$

On the right hand side of these equations, $Z_w(t)$, $K_w(t)$, $M_w(t)$ describe the wave external excitation in the heave, roll and pitch modes, respectively. In the left hand side of the equations, nonlinear restoring terms include dependence on all body modes (z, ϕ, θ) and wave profile (ζ). Dots refer to velocities; double dots to accelerations. In all modes, coefficients with dotted and double dotted subscripts are damping and added masses coefficients, respectively.

In the numerical implementation of this mathematical model added masses, vertical motions dampings, and wave external excitations are assumed linear and are computed using the strip method theory. Roll damping is computed based on Ikeda's method as described by Himeno (1981); restoring actions are taken into account considering multivariable Taylor series (up to the third order) coupling the heave, roll and pitch motions, and the wave profile passing along the ship, representing nonlinear Froude-Krilov effects. The restoring coefficients employed here (see Tables 2 to 6) were analytically derived by Rodríguez (2004). These correspond to an ample generalization of the work of Paulling (1961).

Table 2. Hydrostatic restoring coefficients (calm water): Linear

$Z_z=\rho g A_o$	$K_z=0$	$M_z=-\rho g A_o x_{fo}$
$Z_\phi=0$	$K_\phi=\rho g\left[\nabla_0(\bar z_{B0}-\bar z_G)+I_{xx0}\right]$	$M_\phi=0$
$Z_\theta=-\rho g A_o x_{fo}$	$K_\theta=0$	$M_\theta=\rho g\left[\nabla_0(\bar z_{B0}-\bar z_G)+I_{yy0}\right]$

Table 3. Hydrostatic restoring coefficients (calm water): second order

$Z_{zz}=-2\rho g\int_L \frac{\partial\bar y}{\partial\bar z}dx$	$K_{zz}=0$	$M_{zz}=2\rho g\int_L \bar x\frac{\partial\bar y}{\partial\bar z}dx$
$Z_{z\phi}=0$	$K_{z\phi}=-2\rho g\int_L \bar y^2\frac{\partial\bar y}{\partial\bar z}dx$	$M_{z\phi}=0$
$Z_{z\theta}=2\rho g\int_L \bar x\frac{\partial\bar y}{\partial\bar z}dx$	$K_{z\theta}=0$	$M_{z\theta}=-2\rho g\int_L \bar x^2\frac{\partial\bar y}{\partial\bar z}dx$
$Z_{\phi\phi}=-2\rho g\int_L \bar y^2\frac{\partial\bar y}{\partial\bar z}dx$	$K_{\phi\phi}=0$	$M_{\phi\phi}=2\rho g\int_L \bar x\bar y^2\frac{\partial\bar y}{\partial\bar z}dx$
$Z_{\phi\theta}=0$	$K_{\phi\theta}=2\rho g\int_L x\bar y^2\frac{\partial\bar y}{\partial\bar z}dx$	$M_{\phi\theta}=0$
$Z_{\theta\theta}=-2\rho g\int_L \bar x^2\frac{\partial\bar y}{\partial\bar z}dx$	$K_{\theta\theta}=0$	$M_{\theta\theta}=2\rho g\int_L \bar x^3\frac{\partial\bar y}{\partial\bar z}dx$

Table 4. Hydrostatic restoring coefficients (calm water): third order

Heave

$Z_{zzz}=0$ *	$Z_{zz\phi}=0$	$Z_{zz\theta}=0$ *
$Z_{\phi\phi z}=\rho g\left[4\int_L \bar y\left(\frac{\partial\bar y}{\partial\bar z}\right)^2dx+A_o\right]$	$Z_{\phi\phi\phi}=0$	$Z_{\phi\phi\theta}=-\rho g\left[4\int_L \bar x\bar y\left(\frac{\partial\bar y}{\partial\bar z}\right)^2dx+A_o x_{fo}\right]$
$Z_{\theta\theta z}=0$ *	$Z_{\theta\theta\phi}=0$	$Z_{\theta\theta\theta}=-2\rho g A_0 x_{f0}$ *

Roll

$K_{zzz}=0$	$K_{zz\phi}=\rho g\left[4\int_L \bar y\left(\frac{\partial\bar y}{\partial\bar z}\right)^2dx+A_o\right]$	$K_{zz\theta}=0$
$K_{\phi\phi z}=0$	$K_{\phi\phi\phi}=\rho g\left[8\int_L \bar y^3\left(\frac{\partial\bar y}{\partial\bar z}\right)^2dx+2I_{xxo}-\nabla_0\bar z_{B0}+\nabla_0\bar z_G\right]$	$K_{\phi\phi\theta}=0$
$K_{\theta\theta z}=0$	$K_{\theta\theta\phi}=\rho g\left[4\int_L \bar x^2\bar y\left(\frac{\partial\bar y}{\partial\bar z}\right)^2dx+I_{yyo}\right]$	$K_{\theta\theta\theta}=0$

Pitch

$M_{zzz}=0$*	$M_{zz\phi}=0$	$M_{zz\theta}=0$*
$M_{\phi\phi z}=-\rho g\left[4\int_L \bar x\bar y\left(\frac{\partial\bar y}{\partial\bar z}\right)^2dx+A_o x_{fo}\right]$	$M_{\phi\phi\phi}=0$	$M_{\phi\phi\theta}=\rho g\left[4\int_L \bar x^2\bar y\left(\frac{\partial\bar y}{\partial\bar z}\right)^2dx+I_{yyo}\right]$
$M_{\theta\theta z}=0$*	$M_{\theta\theta\phi}=0$	$M_{\theta\theta\theta}=\rho g\left[2I_{yy0}-\nabla_0\bar z_{B0}+\nabla_0\bar z_G\right]$*

Coupled heave-roll-pitch

$Z_{z\phi\theta}=0$	$K_{z\phi\theta}=-\rho g\left[4\int_L \bar x\bar y\left(\frac{\partial\bar y}{\partial\bar z}\right)^2dx+A_o x_{fo}\right]$	$M_{z\phi\theta}=0$

* Obtained analytically for a wedge-sided ship. It is a good approximation for ships of conventional forms, small displacements and smooth transversal curvatures ($\partial^2\bar y/\partial\bar z^2\to 0$) at the considered water-line.

Table 5. Derivatives due to wave passage: second order Froude-Krilov

$Z_{\zeta z}(t)=2\rho g\int_L \frac{\partial \overline{y}}{\partial \overline{z}}\zeta dx$	$K_{\zeta z}(t)=0$	$M_{\zeta z}(t)=-2\rho g\int_L \overline{x}\frac{\partial \overline{y}}{\partial \overline{z}}\zeta dx$
$Z_{\zeta\phi}(t)=0$	$K_{\zeta\phi}(t)=2\rho g\int_L \overline{y}^2\frac{\partial \overline{y}}{\partial \overline{z}}\zeta dx$	$M_{\zeta\phi}(t)=0$
$Z_{\zeta\theta}(t)=-2\rho g\int_L \overline{x}\frac{\partial \overline{y}}{\partial \overline{z}}\zeta dx$	$K_{\zeta\theta}(t)=0$	$M_{\zeta\theta}(t)=2\rho g\int_L \overline{x}^2\frac{\partial \overline{y}}{\partial \overline{z}}\zeta dx$

Table 6. Derivatives due to wave passage: third order Froude-Krilov

Heave		
$Z_{\zeta\zeta z}(t)=0$ *	$Z_{\zeta\zeta\phi}(t)=0$	$Z_{\zeta\zeta\theta}(t)=0$ *
$Z_{\zeta z z}(t)=0$ *	$Z_{\zeta z\phi}(t)=0$	$Z_{\zeta z\theta}(t)=0$ *
$Z_{\phi\phi\zeta}(t)=-\rho g\int_L\left[2\overline{y}\left(\frac{\partial \overline{y}}{\partial \overline{z}}\right)^2+\overline{y}\right]\zeta dx$	$Z_{\theta\theta\zeta}(t)=0$ *	$Z_{\zeta\phi\theta}(t)=0$
Roll		
$K_{\zeta\zeta z}(t)=0$	$K_{\zeta\zeta\phi}(t)=\rho g\int_L\left[2\overline{y}\left(\frac{\partial \overline{y}}{\partial \overline{z}}\right)^2+\overline{y}\right]\zeta^2 dx$	$K_{\zeta\zeta\theta}(t)=0$
$K_{\zeta z z}(t)=0$	$K_{\zeta z\phi}(t)=-\rho g\int_L\left[4\overline{y}\left(\frac{\partial \overline{y}}{\partial \overline{z}}\right)^2+2\overline{y}\right]\zeta dx$	$K_{\zeta z\theta}(t)=0$
$K_{\phi\phi\zeta}(t)=0$	$K_{\theta\theta\zeta}(t)=0$	$K_{\zeta\phi\theta}(t)=\rho g\int_L\left[4\overline{xy}\left(\frac{\partial \overline{y}}{\partial \overline{z}}\right)^2+2\overline{xy}\right]\zeta dx$
Pitch		
$M_{\zeta\zeta z}(t)=0$ *	$M_{\zeta\zeta\phi}(t)=0$	$M_{\zeta\zeta\theta}(t)=0$ *
$M_{\zeta z z}(t)=0$ *	$M_{\zeta z\phi}(t)=0$	$M_{\zeta z\theta}(t)=0$ *
$M_{\phi\phi\zeta}(t)=\rho g\int_L\left[2\overline{xy}\left(\frac{\partial \overline{y}}{\partial \overline{z}}\right)^2+\overline{xy}\right]\zeta dx$	$M_{\theta\theta\zeta}(t)=0$ *	$M_{\zeta\phi\theta}(t)=0$

* Same hypothesis are applied as in the case of the hydrostatics derivatives in calm water.

The Authors postulate that these analytically derived coefficients are important in the sense of bridging the complicated dynamics of the coupled nonlinear equations of motion with basic hull design characteristics. As will be shown next, for certain hull forms and motions of moderate and high amplitudes, nonlinear restoring actions of higher order play an important role in the dynamic behaviour.

3.2 Numerical Simulations of Roll Amplifications in Head Seas

The strong parametric excitations observed in the experimental results of TS ship are not possible to be reproduced numerically using the classical Mathieu modelling. The essential hypothesis here is that this is due to strong non-linear couplings among vertical motions, roll motion and wave passage effects associated with nonlinear Froude-Krilov terms. Using the new model, we try to identify the influence of the restoring coefficients on parametric excitation, and therefore, on the behaviour of those similar, and at the same time different ship hulls, due to their distinct stern arrangements. Figures 4, 5 and 6 illustrate the good agreement obtained in the comparisons between experimental results and numerical simulations, in cases of low *GM* and steep waves. These figures also demonstrate that the second order model fails to follow the experimental trends.

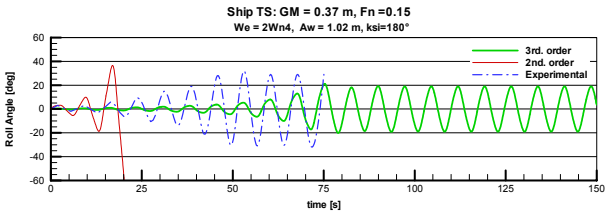

Figure 4 Roll response, Fn=0.15, A_w=1.09 m.

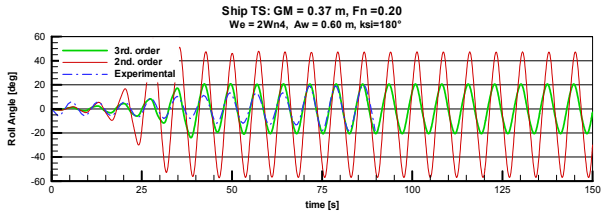

Figure 5 Roll response, Fn=0.20, A_w=0.60 m.

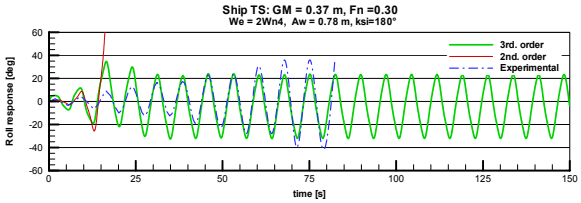

Figure 6 Roll response, Fn=0.30, A_w=0.78 m.

3.3 Numerical Simulations of Heave and Pitch Motions

In head seas, the heave and pitch motions are very important in favouring the occurrence of roll parametric amplification. For small

wave amplitudes, these motions are typically linear. Yet, for larger waves, these motions may loose this character, and asymmetries may be noticed and become remarkable.

Figures 7 and 8 show simulations of the heave and pitch motions for the RS hull in head seas. Results from the third order model are plotted against the linear response for a high wave, A_w=1.0m, Fn=0.10. Similar plottings are shown in Figures 9 and 10 for the TS hull, in this case at a slightly higher ship speed. Comparing the results shown in these figures, it is concluded that the linear responses for the two ships are very similar, being slightly higher for the RS hull, mainly in the case of the pitch motion. Considering the nonlinear simulations, some marked asymmetries are observed in the responses of both modes for the TS hull (again particularly in the case of the pitch motion), making it clear that the heave and pitch motions are not linear anymore.

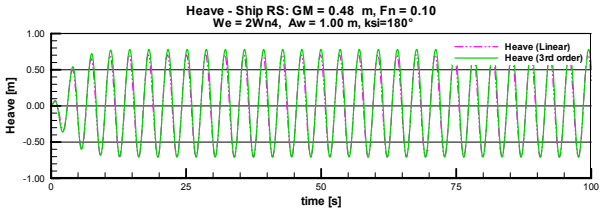

Figure 7 Heave motion in head seas for RS.

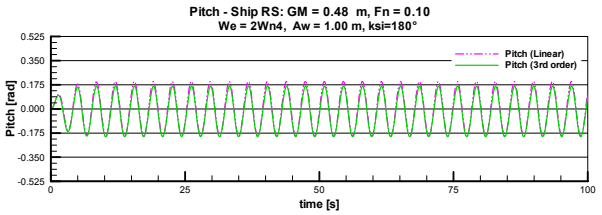

Figure 8 Pitch motion in head seas for RS.

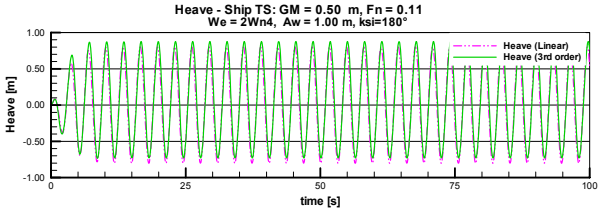

Figure 9 Heave motion in head seas for TS.

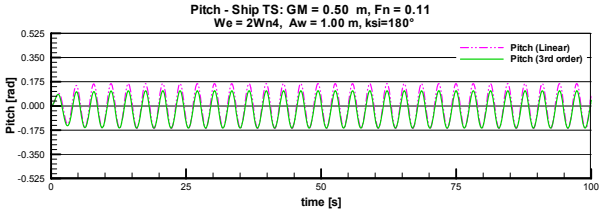

Figure 10 Pitch motion in head seas for TS.

These asymmetric responses point out to the fact that the exchange of energy between the vertical modes and the roll motion, which is an essential aspect of the dynamics of parametric resonance in head seas, must be described as a set of coupled equations, if all the complexities of excessive motions are to be taken into consideration.

The third order couplings are relevant not only in establishing the above observed asymmetries, but also, as will be discussed later, they will give rise to a hardening effect in the roll motion.

3.4 Comparative analysis of restoring terms

For the TS and RS ships the calm-water restoring coefficients for the tested conditions are shown in Table 7.

Table 7. Calm-water restoring coefficients for TS and RS ships

Roll Coeff.	TS		RS	
	***GM* = 0.37 m**	***GM* = 0.50 m**	***GM* = 0.34 m**	***GM* = 0.48 m**
$K_{z\phi}$	-2471		-1225	
$K_{\phi\theta}$	-11195		-1939	
$K_{zz\phi}$	4298		1875	
$K_{\theta\theta\phi}$	289818		76853	
$K_{z\phi\theta}$	25665		3617	
K_{ϕ}	669.8	905.2	574.0	810.4
$K_{\phi\phi\phi}$	-728.9	-860.1	287.2	228.9
$K_{5\phi}$ (*)	330.2	493.8	-936.2	-888.8
$K_{7\phi}$ (*)	-206.7	-288.8	337.0	310.9

(*) Due to the shape of the static stability curve in these conditions, it was necessary to use a higher-order fitting polynomial in the numerical simulations.

As can be seen from Table 1, although TS and RS ships have very similar characteristics, Table 7 shows that they display large differences when comparing their corresponding coupling coefficients. It is noticed that the TS hull has stronger coupling coefficients. Looking at the expressions given in Tables 2 to 6 and Figure 11, it is possible to come out with an explanation for these marked differences: TS hull, due to its transom stern configuration displays much larger longitudinal asymmetry in flare distribution than the RS hull. Therefore, keeping in mind that the coupling coefficients govern the internal transfer of energy between the motions involved, it may be concluded that the TS hull is a more efficient converter of energy from vertical modes to roll motion.

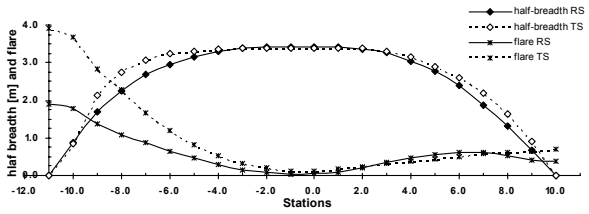

Figure 11 Long'l distribution of half-breadth and flare at waterline for the two hulls.

3.5 The restoring actions and the parametric excitation in roll

We attempt in the following to interpret the essential characteristics of the mathematical model introduced in the previous paragraphs. For the sake of simplicity, we will focus our analysis on the roll restoring moment, $C_\phi(t)$:

$$C_\phi(t) = K_\phi\phi + K_{z\phi}z\phi + K_{\phi\theta}\phi\theta + \frac{1}{2}K_{zz\phi}z^2\phi + \frac{1}{6}K_{\phi\phi\phi}\phi^3 + \frac{1}{2}K_{\theta\theta\phi}\theta^2\phi + K_{z\phi\theta}z\phi\theta + K_{\zeta\phi}(t)\phi + K_{\zeta\zeta\phi}(t)\phi + K_{\zeta z\phi}(t)z\phi + K_{\zeta\phi\theta}(t)\phi\theta$$

To have a better understanding of the roll parametric excitation described by the third-order proposed model, let's assume that there is no roll external excitation (longitudinal waves) and that the heave and pitch motions are harmonic and have linear dependence on wave amplitude. Then, the roll equation becomes uncoupled and after adequate arrangement, it can be expressed in the following form:

$$(J_x + K_{\ddot\phi})\ddot\phi + K_{\dot\phi}(\dot\phi) + K_\phi\phi + \left[A_w^2c_0 + A_wc_1\cos(\omega_e t + \tau_1) + A_w^2c_2\cos(2\omega_e t + \tau_2) + K_{\phi\phi\phi}\phi^2\right]\phi = 0$$

As a consequence of the introduction of third order terms, two additional terms have appeared in the restoring moment: one that gives a bi-harmonic time dependent restoring, and a non-oscillatory term proportional to wave amplitude squared, which can be treated as an additional (nonlinear) stiffness of the dynamical system. Now, it becomes evident that the uncoupled roll motion equation does not correspond anymore to a Mathieu-Duffing equation, but it may be cast as a Hill's differenttial equation.

The nonlinear Froude-Krilov roll moments $K_{\zeta\phi}(t)\phi$ (second order), $K_{\zeta\zeta\phi}$ $(t)\phi$, $K_{\zeta z\phi}(t)z\phi$, $K_{\zeta\phi\theta}\phi\theta$ (third order) are related to the undisturbed incident wave pressure. In longitudinal waves, head seas, the equation of wave surface elevation is:

$$\zeta(x,t) = A_w Cos\left[kx + \omega_e t\right]$$

These nonlinear coefficients (in fact, periodic functions) may be expressed in terms of their cosine and sine terms, such that their dependence on wave amplitude becomes explicit. Thus, for example, the second order term $K_{\zeta\phi}(t)$, proportional to the wave amplitude, may be expressed as:

$$K_{\zeta\phi}(t) = A_w\left[K_{\zeta\phi c}Cos(\omega_e t) + K_{\zeta\phi s}Sin(\omega_e t)\right]$$

The third order terms $K_{\zeta z\phi}(t)$ and $K_{\zeta z\theta}$, also proportional to wave amplitude, are expressed as:

$$K_{\zeta z\phi}(t) = A_w\left[K_{\zeta z\phi c}Cos(\omega_e t) + K_{\zeta z\phi s}Sin(\omega_e t)\right]$$
$$K_{\zeta\phi\theta}(t) = A_w\left[K_{\zeta\phi\theta c}Cos(\omega_e t) + K_{\zeta\phi\theta s}Sin(\omega_e t)\right]$$

It must be observed that the role of these two functions is to parametrically excite the coupled system, appearing multiplied by $z(t)$

and $\theta(t)$, respectively, which on their turn are also periodic functions dependent on wave amplitude. The third order term $K_{\zeta\zeta\theta}(t)$, proportional to wave amplitude squared, is:

$$K_{\zeta\zeta\phi}(t) = A_w^2\left[K_{\zeta\zeta\phi 0} + K_{\zeta\zeta\phi c}Cos(2\omega_e t) + K_{\zeta\zeta\phi s}Sin(2\omega_e t)\right]$$

where it should be observed that it is composed of a constant plus a super-harmonic with double the encounter frequency.

Of particular interest to the present discussion is the nonlinear stiffness, see also Neves and Rodríguez (2004):

$$\begin{aligned} c_0 = {} & \frac{1}{4}K_{zz\phi}\eta_3^2 + \frac{1}{4}K_{\theta\theta\phi}\eta_5^2 + \frac{1}{2}K_{z\phi\theta}\eta_3\eta_5 Cos(\alpha_z - \alpha_\theta) \\ & + \frac{\eta_3}{2}\left[K_{\zeta z\phi c}Cos(\alpha_z) - K_{\zeta z\phi s}Sen(\alpha_z)\right] \\ & + \frac{\eta_5}{2}\left[K_{\zeta\theta\phi c}Cos(\alpha_\theta) - K_{\zeta\theta\phi s}Sen(\alpha_\theta)\right] + K_{\zeta\zeta\phi 0} \end{aligned}$$

where the heave and pitch harmonic motions have been defined as:

$$z(t) = A_w\eta_3\cos(\omega_e t + \alpha_z); \qquad \theta(t) = A_w\eta_5\cos(\omega_e t + \alpha_\theta)$$

The amplitudes of the contributions of the different restoring terms ($R_0 = A_w^2 c_0$, $R_1 = A_w c_1$, $R_2 = A_w^2 c_2$) in the case of RS and TS ships are plotted in Figures 12 to 15 in the frequency domain for two different speeds. The vertical dashed lines indicate the encounter frequencies at which the models were tested.

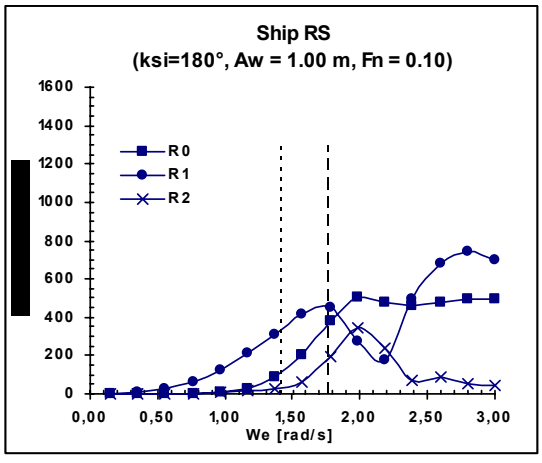

Figure 12 R_0, R_1, R_2 for RS at low speed.

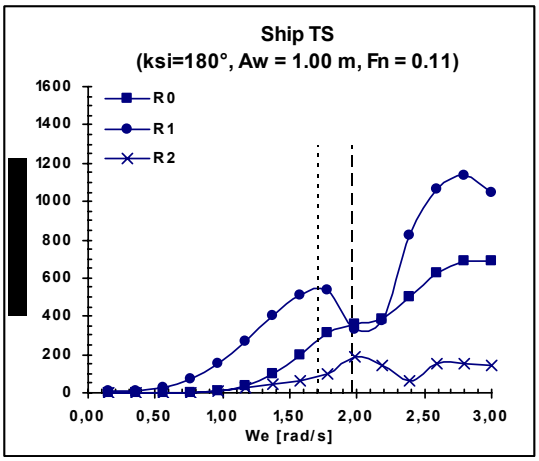

Figure 13 R_0, R_1, R_2 for TS at low speed.

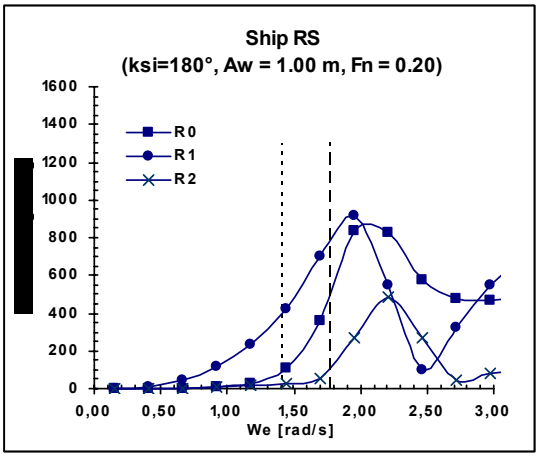

Figure 14 R_0, R_1, R_2 for RS at high speed.

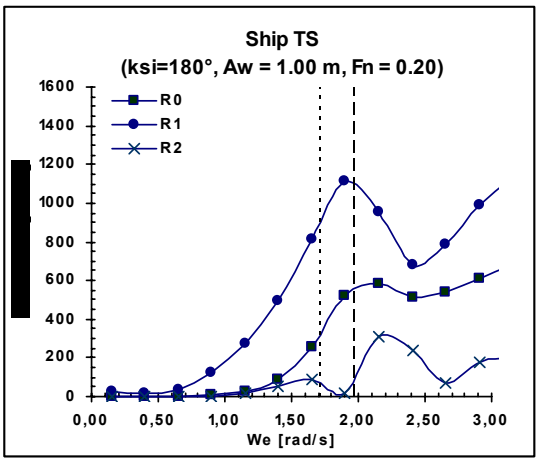

Figure 15 R_0, R_1, R_2 for TS at high speed.

The dependence of R_0, R_1, R_2 on speed is complex, as seen in the corresponding figures, because it not only involves higher responses in the vertical modes at higher speeds, but also displacements of the maximum responses of these motions (heave and pitch) in the encoun-

ter frequency domain, which is reflected in the R_0, R_1, and R_2 encounter frequency spectra. The influence of speed on head seas parametric amplification in the context of the present nonlinear mathematical model has been discussed in greater detail in Neves and Rodríguez (2005).

Finally, another consequence of the hardening effect may be appreciated looking at the new limits of stability, derived in Neves and Rodríguez (2004). These are illustrated in Figures 16 and 17 in the case of a non-dissipative model. Limits of stability for the two hulls are compared. A backbone curve may be traced, reflecting the nonlinear stiffness given above (parabolic curve). Additionally, an upper frontier for the unstable region is observed, which reflects the fact that the nonlinear stiffness causes a detuning of the amplification.

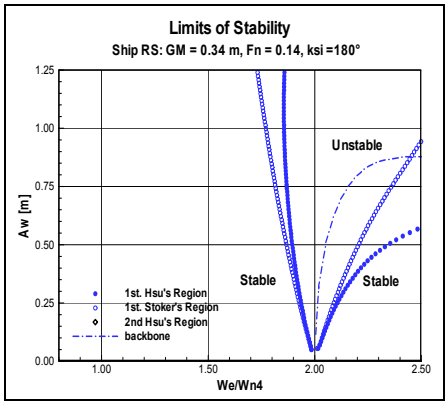

Figure 16 Limits of stability for ship RS, *GM*=0.34 m, *Fn*=0.14

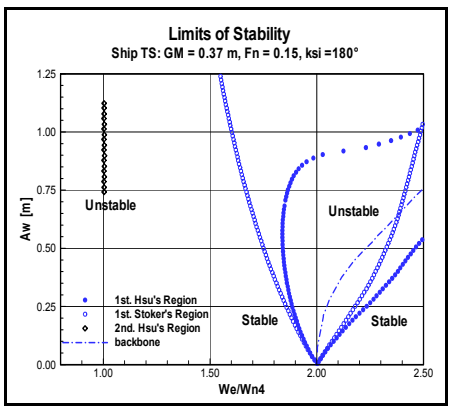

Figure 17 Limits of stability for ship TS, *GM*=0.37 m, *Fn*=0.15.

When damping is introduced, the area of instability within the limits is accordingly reduced, as is illustrated in Figure 18 for the TS hull. The second region of instability, which was merely a vertical trace, now completely vanishes.

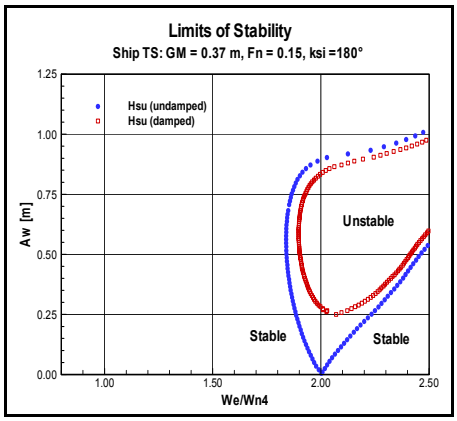

Figure 18 Influence of damping on the limits of stability, ship TS, *GM*=0.37 m, *Fn*=0.15

4. CONCLUSIONS

The following conclusions may be drawn:

A nonlinear mathematical model contemplating terms defined up to the third order in the wave amplitude has been introduced, coupling the heave, roll and pitch modes. Coupling coefficients have been analytically derived, expressed in terms of basic geometric hull characteristics.

Dynamic behaviours of two similar hulls have been compared. Numerical simulations of strong roll resonances have shown good agreement with experimental results. Simulations of the heave and pitch motions in head seas indicated the appearance of asymmetric motions in the case of the TS hull. It has been demonstrated that the nonlinear couplings are much stronger in the case of the TS hull.

Considering the linear variational equation of the nonlinear roll equation, two new contributions, in addition to the harmonic parametric excitation, have been identified: a

bi-harmonic internal excitation, and an additional (nonlinear) stiffness. Analytic expressions have been derived for these contributions.

Terms R_0 and R_2 vary with wave amplitude squared, while R_1 depends linearly on A_w. In general, the prevailing term is the harmonic parametric excitation R_1, whereas much less important is the bi-harmonic internal excitation. However, it is important to notice that as wave amplitude increases, contributions of R_0 and R_2 become more important, and can eventually modify the expected behaviour of the dynamic system.

Considering the behaviour of R_0, R_1, R_2 with wave amplitude, speed and encounter frequency, along with the linear (natural) stiffness of the system and damping, the scenario becomes quite complex and deserves a particular study for each single condition. Nevertheless, this paper has put on evidence the existence of the nonlinear stiffness and bi-harmonic excitation, which may help the understanding of some apparently "contradictory" experimental results. Limits of stability incorporating the third order terms have been discussed.

5. ACKNOWLEDGMENTS

The present investigation is supported by CNPq within the STAB project (Nonlinear Stability of Ships). The authors also acknowledge financial support from Lab-Oceano-COPPE/UFRJ, CAPES and FAPERJ.

6. REFERENCES

France, W.N., Levadou, M., Treakle, T.W., Paulling, J.R., Michel, R.K., Moore, C., 2003, "An Investigation of Head-Sea Parametric Rolling and its Influence on Container Lashing Systems", Marine Technology, vol. 40, no. 1 (Jan), pp. 1-19.

Himeno, Y., 1981, "Prediction of Ship Roll Damping – State of the Art", Report no. 239, Dept. Naval Architecture and Marine Engineering, The University of Michigan.

Luth, H.R., and Dallinga, R.P., 1999, "Prediction of Excessive Rolling of Cruise Vessels in Head and Following Waves", PRADS Conference.

Neves, M.A.S., Pérez, N., Lorca, O., 2002, "Experimental Analysis on Parametric Resonance for Two Fishing Vessels in Head Seas", Proceedings of 6th International Ship Stability Workshop, Webb Institute, New York.

Neves, M.A.S. and Rodríguez, C., 2004, "Limits of Stability of Ships Subjected to Strong Parametric Excitation in Longitudinal Waves", Proceedings of International Maritime Conference on Design for Safety, Osaka, pp. 139-145.

Neves, M.A.S. and Rodríguez, C., 2005, "Stability of Fishing Vessels Subjected to Strong Parametric Excitation", Proceedings of HydMan 2005, Ostróda-Gdansk.

Palmquist, M., and Nygren, C., 2004, "Recordings of Head-sea Parametric Rolling on a PCTC", Annex of Report of Document SLF 47/6/6-IMO.

Paulling, J.R., 1961, "The Transverse Stability of a Ship in a Longitudinal Seaway", Journal of Ship Research, vol. 4, pp. 37-49.

Rodríguez, C., 2004, "Dynamic Stability of Ships – A Third Order Nonlinear Model", M.Sc. Thesis, COPPE/UFRJ. (in Portuguese)

Umeda, N., Hashimoto, H., Vassalos, D., Urano, S., Okou, K., 2003, "Non-Linear Dynamics on Parametric Roll Resonance with Realistic Numerical Modeling", Proceedings of 8th International Conf. on the Stability of Ships and Ocean Vehicles (STAB'2003), Madrid, pp. 281-290.